Thermodynamic uncertainty relation constraints information transmission through cell signaling systems

Shreyansh Verma, Vishva Saravanan R, Bhaswar Ghosh*

Center for Computational Natural Sciences and Bioinformatics,

International Institute of Information Technology, Hyderabad, India

ABSTRACT

Biological systems in general operates out of equilibrium which demands the requirement for constant supply of energy due to non-equilibrium entropy production. The thermodynamic uncertainty relation (TUR) essentially imposes a bound on minimum current fluctuation the system can have given a entropy production rate. The fluctuation eventually impacts the signal to noise ratio imposing an upper bound on information transmission accuracy. In this study, we explored the role of TUR on the information transmission capacity of a set of cellular signaling systems using a coupled mathematical and machine learning approaches to experimental data in yeast under several stress conditions. Cell signaling systems are involved in sensing the changes in environment by activating a set of transcription factors which typically diffuse inside the nucleus to trigger transcription of the required genes. However, the inherent stochasticity of the biochemical pathways associated with signaling processes severely limits the accuracy of estimating the environmental input by the transcription factors. Application of TUR reveals a general picture about the working principle of the transcription factors. We found that the the activation followed by biased diffusion of transcription factors (TF) towards the nucleus triggers entropy production which amplifies magnitude of the overall TF currents towards the nucleus as well as reduces the fluctuations. These outcomes significantly improve the accuracy of information transmission carried out by the transcription factors following the bound imposed by TUR. Thus, experimental observations coupled with TUR based theoretical models demonstrate the role of thermodynamic fluctuation and entropy production on cellular information processing.

INTRODUCTION

Every living cell is required to sense the environment properly to ensure appropriate phenotypic response. The sensing of the extracellular signal is usually carried out by a receptor on the cell membrane which then triggers a downstream signaling cascade finally leading to the activation of one or more transcription factors. These activated transcription factors then diffuse inside the nucleus to stimulate transcription of several genes which would enable the cell to alter its phenotype appropriate for the environmental signal [1]. The biochemical pathways starting from the signal transduction to the nuclear localization involve inherently stochastic processes giving rise to fluctuation in the transcription factor localization output. These are the basis for noisy response stemming from both intrinsic and extrinsic sources and finally severely limiting the accuracy of estimating the input

* Contact author: bhaswar.ghosh@iiit.ac.in

signal which may lead to inappropriate activation of the downstream genes [2, 3, 4, 5]. Consequently, undesired activation of the genes would not only impact the phenotypic outcome as well as incur unnecessary waste of the cell's valuable resources in terms of material and energy. Thus, accurate estimation of the environmental signal is crucial for the cell to avoid such undesirable outcomes. However, it is also generally established that improving accuracy in input estimation will in turn impose extra burden by enhancing energy dissipation [6, 7, 8, 9]. In fact, the general principle of thermodynamic uncertainty relation (TUR) postulates the need for higher entropy production to improve accuracy by reducing fluctuation in the current in a random walk scenario [10]. The nuclear localization of transcription factors under the influence of environmental stress offers a conducive scenario to explore the principle of TUR in biological context. Previous studies have already alluded to TUR in biology specifically in the context of molecular motors [11]. But, it's application in signal transduction cascades remains unexplored plausibly due to lack of experimental data. In the last few years with the unprecedented advancement of microfluidic devices coupled to high resolution imaging techniques, it is now possible to track localization of individual transcription factors inside a single cell. Recently, an experimental study has been conducted to capture the localization of a set of transcription factors in yeast S. Cerevisiae under multiple different environmental stress and information transmission capacity of the pathways [12].

In this study, we take recourse to these publicly available data sets and first employ information theory techniques to calculate the accuracy of information transmission carried by the nuclear localization of the activated proteins. The change in the output (e.g. stimulated expression of a gene) carries information about the input variable. In general, the precision with which the input value can be estimated from measuring the output improves with larger changes (i.e. dynamic range) of the output and with lower output noise. According to Cramėr–Rao inequality, the error in estimating the input from the output is bounded by the Fisher information, defined as the relative entropy change of the output distribution for an infinitesimal change in the input around a given input value [13]. Furthermore, information transmission capacity of signalling systems can also be estimated by calculating the mutual information, which is increasingly being used to characterize biochemical signalling networks [14, 15, 16, 17, 18, 19, 20]. The mutual information measures the mutual interdependence between the input and the output distributions by calculating the relative entropy of the output distributions conditioned on the input with respect to the unconditioned output distributions. In both cases, more information can be extracted about the input from the output distribution if the relative entropy change is large [21, 22, 23]. In addition to the inherent stochasticity, the underlying reactions involved in biochemical pathways are essentially out of equilibrium processes. The close connection between information and heat dissipation in non-equilibrium processes is established on a strong theoretical footing owing to the resolution of the long standing puzzle of Maxwell's demon through the Landauer erasure principle in the last century [24, 25]. Entropy production rate is the measure of heat dissipation in non-equilibrium processes and entropy production rate also represents the energy consumption in many systems at steady state [26]. The essential phenomena which separates a non-equilibrium process from an equilibrium one is the presence of currents arising from breaking of time reversal symmetry [27, 28, 29]. The entropy production rate can be exactly quantified from the the trajectory of a stochastic processes by calculating current if the underlying equation giving rise to the dynamics is known [30, 31], But, unfortunately the underlying dynamical equations are not known in majority of the cases. One of the alternative strategies is to determine the current fluctuation

from the thermodynamic force by training a neural network model based on trajectory data sets and subsequently estimate a bound on the entropy production rate [32]. Another technique relies on the time reversal symmetry breaking criteria to estimate entropy production rate [33]. This method has the ability to capture hidden entropy production in a trajectory where the current in the trajectory may be very low. This method essentially calculates the forward and reverse transition probabilities between a set of pre-selected states. The selection of the states are later optimized to minimize the entropy production rate using optimization algorithms. Here, we used these methods to estimate the entropy production rates of the trajectories of protein localization along with the calculation of accuracy of information transmission mentioned previously. The information transmission capacity is observed to display a strong correlation with the estimated bound on the entropy production rate expected from the thermodynamic uncertainty relation. We further found that the intrinsic noise in the trajectory shows strong anti-correlation with the entropy production rate. These results imply that the entropy production rate enables reduction in intrinsic noise which in turn improves signal to noise ratio leading to better information transmission accuracy. We further observed that the reduction in intrinsic noise also amplifies the accuracy by dynamic measurement of the output. In fact, a model based on biased random walk of the proteins fundamentally corroborates the analysis of experimental data. Our study offers a general theoretical framework to lay down an underlying mathematical principle of TUR which drives the protein localization through energy dissipation.

RESULTS

Higher response magnitude to the input leads to a lower fluctuation at the output

To explore the role of fluctuation on the response of the biological signaling pathway, we analyzed the single cell measurement of the dynamics of the transcription factor nuclear localization signal under various stresses in the yeast *S. Cerevisiae* [12]. In this experiment, the nuclear localization signal of ten different transcription factors under three different stresses, namely carbon, oxidative, and osmotic stresses, is estimated using fluorescent tagged transcription factors through a microfluidic devise. The nuclear localization is quantified by the ratio of the fluorescent signal within the nucleus to the cytoplasm. The experimental data provide us with the trajectories before and after the stress inside individula cells for each transcription factors (Fig S1). The cell to cell variability in nuclear localization after the treatment of the stress for one of the transcription factors quantifies the noise in the response for that particular transcription factor. The average signal provides a general trend in response of the transcription factors (Fig 1a). To estimate the relationship between the average amplitude and fluctuation, we calculated the mean response at the maximum magnitude for each transcription factor (Fig S1) after the stress is applied and the corresponding variance describes the noise strength. The noise represented by the coefficient of variation ($CV = \frac{variance}{mean^2}$) shows an expected decreasing trend with the maximum average response for the threes different streses (Fig 1b-1c). Thus, as the response is higher the noise in the response is lower. The lower noise as a result would improve the signal-to-noise ratio, leading to an improvement in information transmission.

Improved information transmission due to reduced fluctuation

Information transmission can be quantified by calculating the mutual information between input and output. Mutual information provides a measure of information the output signal carries about the change in the input. As in our case, there are two values of the stresses (eg. in presence and absence of carbon stress) which entails only one bit of information at the input and thus, we would expect the output would carry at most 1 bit of information about the input. However, some information is going to be inevitably lost due to fluctuation arising from stochasticity in the underlying pathway. We used a previously described method to calculate the information [12]. The method utilizes a SVM based classifier to predict the input from the output signal at a particular time point or the entire trajectory (Methods section D). The confusion matrix provides the joint distribution $p(X = x, Y = y)$ of the predicted value x and actual value y which can be used to determine the mutual information between the two variables X and Y following the definition

$$I(X;Y) = \sum_{x,y} p(X = x, Y = y) \log \frac{p(X = x, Y = y)}{p(X = x)p(Y = y)}$$

where $p(X = x)$ and $p(Y = y)$ represent the total probability distribution of X and Y respectively given by

$$p(X = x) = \sum_{y} p(X = x, Y = y)$$

$$p(Y = y) = \sum_{x} p(X = x, Y = y)$$

Using this method, the mutual information is calculated at each time point along trajectory using a sliding time window as indicated in Fig 2a-c for different stress conditions and select the mutual information value where the response is maximum for each transcription factors. The mutual information indeed increases as the response is higher irrespective of the nature of the stress which corroborates our hypothesis that the higher response improves information transmission by reducing the fluctuation for carbon (Fig 2d), osmotic (Fig 2e) and oxidative stresses (Fig 2f) as depicted by correlations (R=0.67,p=0.03 for carbon; R=0.68,p=0.001 for osmotic; R=0.92,p=0.0002 for oxidative) between response amplitude and information.

Higher response enhances the entropy production rate

The thermodynamic uncertainty relation [34] is described by the inequality

$$\frac{Var(J)}{J^2} \geq \frac{2}{\Sigma}$$

where J represents the current through the physical system and Σ corresponds to the entropy production in the system due to the current. The uncertainty relation essentially states that the reduction in fluctuation entails a cost by increasing the entropy production. As in our case, reduction in fluctuation due to amplified response must incur higher entropy production in the nuclear localization process. The entropy production rate can be exactly quantified from the the trajectory of a stochastic processes by calculating current if the underlying equation giving rise to the dynamics is

known, But, unfortunately the underlying dynamical equations are not known in our cases. One of the alternative strategies is to determine the current fluctuation from the thermodynamic force by training a neural network model based on trajectory data sets and subsequently estimate a bound on the entropy production rate [32]. We take recourse to one of the recently developed techniques to estimate the entropy production rate from the trajectory of the nuclear localization signal (Method section E). Following the statement of uncertainty relation, the entropy production rates would be higher at higher response amplitude since fluctuation is lower, leading to the observed correlation between the mutual information and entropy production for the transcription factors over carbon (Fig 3a,R=0.81), osmotic (Fig 3b,R=0.56) and oxidative stresses (Fig 3c,R=0.74).

Entropy production constraints the information transmission by imposing an upper bound

When the environmental input has two possible values, The mutual information between the input and output can be derived as (Methods section A)

$$I = log\left[1 + \frac{J^2}{4Var(J)}\right]$$

where J is the flux through the pathway as defined in the previous section. In view of the uncertainty relation, the information would have an upper bound given by the inequality

$$I \leq log\Big(1 + \Sigma\Big)$$

In fact, this inequality assumes that the time scale of the change in the input and the output are slow so that the pathway relaxes to the steady state along with the input. However, if the time scale of the pathway and the input is different, then one can show using the assumption of linear response (Methods section B) that the inequality takes the form

$$I \leq log\left(1 + \frac{\tau_s}{\tau_p}\Sigma\right)$$

Here, τ_s and τ_p represent the time scale of the change in input stress and the pathway, respectively. In fact, we can observe that as the time scale of the pathway is much slower than the change in the input, the value on the right-hand side would become very low, implying that a very slow pathway would not be able to carry information about a rapidly changing input even though entropy production is high enough. However, the functional form of the upper bound does not change apart from the extra factor. The estimated bounds from the entropy production rates are indeed higher than the mutual information in our case as indicated in the previous figure 2. The algorithm based on neural network as described in the previews section relies on the time reversal symmetry-breaking criteria to estimate the entropy production rate. This method essentially calculates the forward and reverse transition probabilities between a set of pre-selected states. The selection of the states are later optimized to minimize the entropy production rate using optimization algorithms. In fact, the estimated bound in this method is found to be higher than the mutual information, although since it calculates the entropy production also for low flux the correlation between flux and the entropy production rate was not very high. In this method the entropy production rate is calculated

from the trajectory of the experiment which essentially measures the ratio between the nuclear and cytoplasmic protein. Further, the experimental data does not provide us the flux and it's fluctuation through the pathway. The true entropy production as well as the fluctuation in the current can only be calculated if the underlying reaction network is known. In order to estimate entropy production with a more mathematically valid technique, we next take recourse to a mathematical model that essentially captures the pathway.

A mathematical model captures the actual entropy production and current fluctuation

The mathematical model is constructed based on four different states of the protein molecule diffusing in and out of the nucleus [35]. The presence of the signal usually activates the protein by phosphorylation / dephosphorylation to localize / delocalize inside the nucleus (Fig 4a). we next fitted the average trajectory of the ratio of nuclear and cytoplasmic proteins to the experimental trajectory using a genetic algoritm framework (Methods section F) to extract the reaction rates for each transcription factor, as indicated by the example of the fitted curves (Fig 4b for Msn2 and Fig S2 for others). The convergence of the genetic algorithm is displayed by the reduction in the error (Fig S3). In the model, we assumed that the NC ratio reaches a steady state after the stress is applied in order to capture the essential dynamics just after the application of the environmental change. However, in the experiment the transcription factors start to diffuse back to cytoplasm again after some time plausibly due to phenotype changes which is not considered in our model. Finally, a set of Monte Carlo simulation based on Gillespie algorithm (Method section G) is performed for the transcription factors individually. The currents (J_1, J_2, J_3, J_4) trough the reaction pathways and entropy production rate (Σ) are quantified by

$$
\begin{aligned}
J_1 &= (K_1[y_1] - K_2[y_2]) \\
J_2 &= (K_3[y_2] - K_4[y_4]) \\
J_3 &= (K_6[y_2] - K_5[y_3]) \\
J_3 &= (K_7[y_3] - K_8[y_1])
\end{aligned}
$$

$$
\Sigma = J_1 \log \frac{K_1}{K_2} + J_2 \log \frac{K_3}{K_4} + J_3 \log \frac{K_6}{K_5} + J_4 \log \frac{K_7}{K_8}
$$

Here, y_1, y_2, y_3 and y_4 correspond to the average values over many trajectories and additionally at the steady state the currents will be equal to each other ($J_1 = J_2 = J_3 = J_4 = J$). The trajectories generated through the simulation are then used to calculate the mutual information carried by NC ratio ($\frac{y_3+y_4}{y_1+y_2}$) and also fluctuation in the current (J) after the stress is applied which paves the way towards verifying the thermodynamic uncertainty relation. In fact, a decreasing trend in the values of $\frac{var(J)}{J^2}$ with the entropy production rates is observed for all the stresses (Figure 4c) quantified by the negative correlation values (R=-0.79 for carbon, R=-0.77 for osmotic, R=-0.74 for oxidative). The entropy production rates would be higher at higher response amplitude since fluctuation is lower, leading to the observed correlation between the mutual information and entropy production for the transcription factors over carbon, osmotic and oxidative stresses (Figure 4d). as indicated

by the positive correlation values (R=0.67 for carbon, R=0.67 for osmotic, R=0.42 for oxidative). The theoretical value of $log(1+\Sigma)$ is indeed always higher than the information as expected from the inequality. A two-state equivalent version can be constructed in order to calculate the mutual information and entropy production following an analytical framework (Method section C).

$$A(\alpha) = \frac{\alpha^2}{\sigma^2_{R|S}}\left(\frac{\delta R}{\delta \alpha}\right)^2 = \frac{\alpha^2\alpha_1^2\beta}{(\alpha_1\alpha+\alpha_0)(\alpha_1\alpha+\alpha_0+\beta)^2}X_T$$

One can connect the accuracy and mutual information as described in the method section,

$$I = log(SNR) = log\left(1 + A(\alpha)\frac{\Delta\alpha^2}{4\alpha^2}\right)$$

The entropy production rate can be written as,

$$P_{ex}(\alpha) = \sigma = X_T\frac{\beta_{eq}(\alpha_0+\alpha_1\alpha)}{\alpha_0+\alpha_1\alpha+\beta_{eq}}\Delta F$$

The thermodynamic uncertainty relation only imposes an upper bound on the information, but it does not grantee a correlation between information and entropy production. To explore the possibilities, we vary both the values of β and α_1 and calculated the accuracy $A(\alpha)$ and the entropy production rate $P_{ex}(\alpha)$ following the analytical expression above. In fact, the accuracy increases with the entropy production up to some optimum value of $P_{ex}(\alpha)$ after which the accuracy tends to decrease (Fig 5a). The range over which the the correlation is evident depends on the activation rate α_1. For higher values of α_1, the range over which correlation is observed expands at different input values α (Fig 5b). However, at very high α_1 values the accuracy again tend to remain constant over the range (Fig 3c). The analysis suggests that the reactions must operate in the linear response regime at intermediate values of activation rates such that the pathway can fully exploit the entropy production in achieving higher accuracy.

Dynamic measurement marginally improves the performance of the signaling pathway but can not overcome the thermodynamic limit

Till now, we have looked at the information at a single point just after the stress is applied. It has been established previously that dynamic measurement in general improves information transmission in cell signaling pathways by filtering out extrinsic noise [17, 36]. To explore this possibility, we set out to calculate the mutual information by increasing the length of the trajectories starting from the starting time point. For each stresses, the average value of the mutual information over all the transcription factors is calculated to display the average trend. In fact, information sharply increases as the length of the trajectory increases and beyond a point it saturates (Figure 6A). We noticed that beyond a time point of 10, the trajectory has significantly more information compared to single point mutual information as the trajectory keeps information about previous values. We define the performance efficiency as the ratio of the mutual information and entropy produced over the length

of the time value of which is always less than one according to thermodynamic uncertainty relation.

$$\eta = \frac{I}{log(1 + n\Sigma)} < 1$$

The performance efficiency described by also exhibits a significant amplification due to dynamic measurement (Figure 6B). However, it is legitimate to compare the efficiency for single time point measurement. The dynamic efficiency is shown to be higher albeit, not with a very large margin at the initial time points but since the essential implication of dynamic measurement is the storage of past information, we observe that the dynamic efficiency is higher with a higher margin at later time points. It should also be kept in consideration that the storage of information would also entail an extra cost in energy consumption proportional to the number of time points to keep in memory. Thus, in view of the result, we can conclude that the dynamic measurement of information provides a marginal advantage to these signaling pathways not a drastic one. This possibly occurs since the pathway outputs are dominated by intrinsic noise at the nuclear localization level. From a evolutionary point of view, the cell one one hand tries to improve the information about the environment but on the other hand do utilize strategies to minimize entropy production either through the signaling cascades or in storage of memory. This conflicting goals pose a challenging optimization landscape to navigate through evolutionary dynamics and possibly offers a fundamental design principle for the biochemical organization.

DISCUSSION

Thermodynamic uncertainty relation essentially establishes connection between the fluctuation and entropy production in far from thermal equilibrium system. This formulation in fact deals with the long standing observation of Maxwell's demon which alluded to a fundamental connection between information and thermodynamics [37]. The thermodynamic uncertainty relation essentially reinforce the connection by constraining the fluctuation in a physical current and power consumption in the system and finally fluctuation's intimate link with information establishes the role of power consumption to information as discussed in our study specifically in the context biological signaling as an example of a physical system [38, 39]. Derivation of the basic uncertainty relation presupposes some assumption for the system namely, stationarity and linear response [40]. In the case we studied the stationarity condition only holds true at the beginning of the application of stress but the pathway activity starts to fall down after some time. In order to establish the validity of the results found from the experimental data, we constructed a mathematical model which essentially takes into account the stationarity condition and we found that the overall claim is not contingent on the non-stationarity at the later part of the pathway activity. In fact, the pathway activity almost becomes very low i.e, close to the equilibrium state after some time which indicates that current as well as entropy production becomes vanishing small in that regime, but the information as measured by the dynamic response is still high, apparently breaking the limits imposed by the uncertainty relation and this was possible since the pathway keeps the past memory in store even after the pathway activity relaxes back to the pre-stress state as we have quantitatively established in the result section. In fact, it is suggested that dynamic measurements of the input signal rely on storage memory capacity of the previous states by the signaling pathway in order to improve accuracy [41].

However, the question still remains unanswered how the memory storage would be achieved by the cell mechanistically. A possible mechanism was suggested in the context of bacterial chemo-taxis where the past memory remains stored in the slow methylation patterns in the receptor where as the phosphorylation signal relaxes back to pre-treatment state [42]. This was achieved through the utilization of an integral negative feedback. In fact, the studies also reinforce the fact that the memory storage through the negative feedback imposed extra energetic cost and cell anchors the feedback loop in order to optimize the energy-accuracy trade-off in scenarios of energy budget constraints [7]. The requirement for optimal resource allocation due to the energy-accuracy trade-off in signaling systems is emerging as a crucial design principle for biological signaling systems in multiple studies [43, 6, 44, 45, 46]. Thus, it should be kept in mind that memory operations would not be attained without an extra resource burden. Our study exhibits the limit to the information transmission in view of the energy cost due to dissipation at steady state and living organism may deal with this trad-off in multiple ways either by reducing the ATP consumption in signaling cascade which will increase fluctuation degrading information transmission, or introducing feedback loop or storing past information as memory while shutting down the pathway output. More experimental coupled with theoretical frameworks are needed to explore which strategy is appropriate in different scenarios.

According to Landauer's principle [24], the work done during a thermodynamic cycle occurs due to erasure of memory but not storage of memory. So, if the systems has enough memory without the requirement for erasure the extra burden can be overcome. But, of course the memory storage capacity must be maintained without degeneration which is a long term burden. We would like to argue that the the limits due to uncertainty relation can be overcome through memory storage in the short term as long as the memory storage capacity does not get corrupted during the time. In analogy with a computer, the hard disk can store information in it's memory without any extra cost as long as the hard disk remains uncorrupted. It is another matter which needs to be explored that how biological system can achieve memory storage dynamically as exemplified in case of bacterial chemotaxis. At least, biological systems do store information at the level of DNA but how is it going to to it at the signaling levels needs more exploration. Our study offers a mathematical framework to observe how biological systems deal with the limits imposed by non-equilibrium thermodynamics on the performance of their operation.

MATERIALS AND METHODS

A. Bound on mutual information

If $P(R,S)$ is the joint distribution of the response R and signal S, total variance of the response [17]

$$\sigma_R^2 = \int R^2 P(R,S) dR dS - \left[\int RP\left(R,S\right) dR dS\right]^2$$

Conditional Variance

$$\sigma_{R|S}^2 = \int \left[\int R^2 P(R|S) dR - \left[\int RP(R|S) dR\right]^2\right] P(S) dS$$

$$= R^2 R(R|S)dRdS - \int \left[\int RP(R|S)dR\right]^2 R(S)dS$$

Thus,

$$\sigma_R^2 = \sigma_{R|S}^2 + \int \left(\int RP(R|S)dR\right)^2 P(S)dS - \left(\int RP(R|S)dRdS\right)^2$$

If there are two inputs S_1 and S_2

$$\sigma_R^2 = \sigma_{R|S}^2 + \frac{1}{2}\left(\langle R_1\rangle^2 + \langle R_2\rangle^2\right) - \left(\frac{1}{2}\langle R_1\rangle + \frac{1}{2}\langle R_2\rangle\right)^2$$

Where,

$$\langle R_1\rangle = \int RP(R|S_1)dR.$$

$$\langle R_2\rangle = \int RP(R|S_2)dR.$$

$$p(S_1) = \frac{1}{2} \quad \text{and} \quad p(S_2) = \frac{1}{2}$$

$$\sigma_R^2 = \sigma_{R/S}^2 + \frac{1}{4}(\langle R_1\rangle - \langle R_2\rangle)^2$$

$$SNR = \frac{\sigma_R^2}{\sigma_{R/S}^2} = 1 + \frac{(\langle R_1\rangle - \langle R_2\rangle)^2}{4\sigma_{R/S}^2}$$

If we assume that the distributions are Gaussian.
The mutual information

$$I = \log(SNR)$$

If the response is taken as the current through system.

$$SNR = 1 + \frac{(\langle J_1\rangle - \langle J_2\rangle)^2}{4\sigma_{J/S}}$$

We assume that the system is at equilibrium when no stress is applied and it goes out of equilibrium when stress is applied.

$$\langle J_1\rangle = 0$$

$$SNR = 1 + \frac{J^2}{4Var(J)}$$

According to the thermodynamic uncertainty relation

$$\frac{Var(J)}{J^2} \geq \frac{2}{\sum}$$

$$SNR = 1 + \frac{J^2}{4Var(J)} \leq log\left(1 + \sum\right)$$

$$\Rightarrow I = \log\left(1 + \frac{J^2}{4Var(J)}\right) \leq \log\left(1 + \sum\right)$$

B. Analytical expression for upper bound on measurement accuracy

For a non-equilibrium stochastic process of a random variable x, the steady state probability distribution can be denoted by $\rho(x, \alpha)$ where α is the control parameter. Following Hatano-Sasa formulation [47, 48] for transition between non-equilibrium steady states, the non-equilibrium free energy can written as

$$\phi = -log(\rho(x, \alpha)$$

The conjugate force corresponding to the control parameter α is given by

$$X(x, \alpha) = \frac{\delta\phi(x, \alpha)}{\delta\alpha}$$

For a small change in the value of α to $\alpha + \delta\alpha$, the average change in the conjugate force around the steady state value can be derived using linear response theory [49], $\langle \Delta X(t) \rangle_{ss} = \int_{-\infty}^{t} dt' \, \delta\alpha(t') \chi(t - t')$

Where,

$$\chi(t - t') = \frac{d}{dt} \langle X(t) X(t') \rangle_{ss}$$

The thermodynamic internal energy due to the process can be represented as

$$E = \alpha \langle \Delta X \rangle_{ss}$$

and the corresponding excess power generated due to the process is [48]

$$P_{ex} = \frac{d\alpha}{dt} \langle \Delta X \rangle_{ss}$$

By integrating by parts, we can finally get

$$p_{ex}(t) = \left(\frac{d\alpha}{dt} \right)^2 \int_0^\infty dt' \langle X(0) X(t') \rangle_{ss}$$

Following the steps above, it can be shown that,

$$\begin{aligned} p_{ex}(t) &= \left(\frac{d\alpha}{dt} \right)^2 \int_0^\infty dt' \langle X(0) X(t') \rangle_{ss} \\ &= \left(\frac{d\alpha}{dt} \right)^2 \int_0^\infty dt' \langle X(0) X(0) \rangle_{ss} e^{-\gamma t'} \end{aligned}$$

Since, the fisher information F at steady state is defined as,

$$F = \Big\langle X(0) X(0) \Big\rangle = \left\langle \left(-\frac{\delta \log \rho(x, \alpha)}{\delta\alpha} \right)^2 \right\rangle$$

Thus, finally the calculation leads to a power-accuracy trade-off [49].

$$P_{ex} = \frac{F}{\gamma} \left(\frac{d\alpha}{dt} \right)^2$$

According to Cramėr–Rao inequality $var(\alpha) \geq \frac{1}{F}$ which imply that,

$$P_{ex} \geq \frac{1}{(\Delta\alpha)^2\gamma}\left(\frac{d\alpha}{dt}\right)^2 = \frac{\alpha^2}{(\Delta\alpha)^2\gamma}\left(\frac{d\alpha}{\alpha dt}\right)^2$$

$$\frac{A(\alpha)}{P_{ex}(\alpha)} \leq \gamma\tau_\alpha^2$$

Here, $A(\alpha) = \frac{\alpha^2}{(\Delta\alpha)^2}$ is the accuracy of estimating the signal and inverse of $\frac{d\alpha}{\alpha dt}$ represents time scale of the signal change τ_α.

C. Breaking of detailed balance and thermodynamic uncertainty relation

For our case, the cytoplasmic version x_1 and nuclear version x_2 of the transcription factor would follow the dynamics,

$$\frac{dx_2}{dt} = (\alpha_0 + \alpha_1\alpha)X_T - (\alpha_0 + \alpha_1\alpha + \beta)x_2$$

The Langevin equation at steady state is,

$$\frac{d\Delta x}{dt} = -(\alpha_0 + \alpha_1\alpha + \beta)\Delta x + \eta(t)$$

The steady state distribution around the steady state is given by,

$$\rho(x, \alpha) = \frac{1}{\sqrt{2\pi\sigma^2}}e^{-(x-\mu)^2/2\sigma^2}$$

The response and variance at steady state are given by,

$$R = \frac{\alpha_0 + \alpha_1\alpha}{\alpha_0 + \alpha_1\alpha + \beta}X_T;\ \sigma^2_{R|S} = \frac{(\alpha_0 + \alpha_1\alpha)\beta}{(\alpha_0 + \alpha_1\alpha + \beta)^2}X_T$$

The accuracy [8, 6] is the fisher information with respect to the input α and if we assume that total number of the sensing molecule X_T is large (Supplementary information), it can be shown to be given by ,

$$A(\alpha) = \frac{\alpha^2}{\sigma^2_{R|S}}\left(\frac{\delta R}{\delta\alpha}\right)^2 = \frac{\alpha^2\alpha_1^2\beta}{(\alpha_1\alpha + \alpha_0)(\alpha_1\alpha + \alpha_0 + \beta)^2}X_T$$

One can connect the accuracy and SNR as described in the previous section,

$$SNR = \frac{\sigma_R^2}{\sigma^2_{R/S}} = 1 + \frac{(\langle R_1\rangle - \langle R_2\rangle)^2}{4\sigma^2_{R/S}} = 1 + \frac{\Delta\alpha^2}{4\sigma^2_{R|S}}\left(\frac{\delta R}{\delta\alpha}\right)^2 = 1 + A(\alpha)\frac{\Delta\alpha^2}{4\alpha^2}$$

In the previous section, we assumed an expression of the power consumption, and in this section, we are providing a derivation of the expression from the entropy production rate in case of the chemical reaction system when detailed balance is broken.

For the chemical reaction system described above, the transitions between the two states are driven by an external force due to the enzyme *alpha* in addition to the equilibrium transition rates α_{eq} and β_{eq}. External driving breaks the detailed balance of the cycle, leading to the entropy production rate and power consumption by the cycle [50]. The steady state is given by

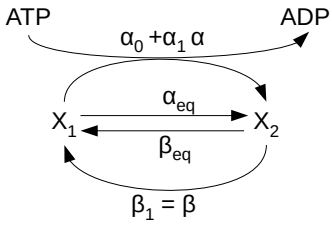

$$X_2 = \mu = \frac{\alpha_0 + \alpha_1\alpha + \alpha_{eq}}{\alpha_0 + \alpha_1\alpha + \alpha_{eq} + \beta_{eq} + \beta_1} X_T$$

The corresponding entropy production rate is,

$$\sigma = [(\alpha_0 + \alpha_1\alpha)X_1 - \beta_1 X_2] log \frac{\alpha_0 + \alpha_1\alpha}{\beta_1} + [\alpha_{eq}X_1 - \beta_{eq}X_2] log \frac{\alpha_{eq}}{\beta_{eq}}$$

At steady state, the fluxes would be equal

$$(\alpha_0 + \alpha_1\alpha)X_1 - \beta_1 X_2 = -(\alpha_{eq}X_1 - \beta_{eq}X_2)$$

This essentially breaks the detail balance as the fluxes are not individually zero which responsible for the net fluxes and the emergence of a nonzero entropy production rate at steady state. Thus, finally the expression for the flux is given by,

$$J = X_T \frac{(\alpha_0 + \alpha_1\alpha)\beta_{eq} - \alpha_{eq}\beta_1}{\alpha_{eq} + \alpha_0 + \alpha_1\alpha + \beta_1 + \beta_{eq}}$$

One can show that, assuming $\alpha_0 = 0$

$$\frac{(\Delta J)^2}{J^2} = \frac{(\beta + \beta_{eq})^2(\alpha_{eq} + \beta_{eq})^2}{\beta_{eq}^2\left(\alpha - \frac{\alpha_{eq}\beta}{\alpha_1\beta_{eq}}\right)^2}(\Delta\alpha)^2$$

which implies

$$\frac{(\Delta J)^2}{J^2} \geq \frac{(\Delta\alpha)^2}{\alpha^2}$$

Finally, the thermodynamic uncertainty relation for a changing environment is given by

$$\frac{(\Delta J)^2}{J^2} \geq \frac{\tau_s}{\tau_\alpha \Sigma}$$

The entropy production rate is given by

$$\sigma = X_T \frac{(\alpha_0 + \alpha_1\alpha)\beta_{eq} - \alpha_{eq}\beta_1}{\alpha_e q + \alpha_0 + \alpha_1\alpha + \beta_1 + \beta_{eq}} log \frac{\alpha_0 + \alpha_1\alpha}{\beta_1} \frac{\beta_{eq}}{\alpha_{eq}}$$

The external driving force exerted by the enzyme α associate a free energy F to the reaction in addition to the equilibrium free energy E. Thus one can associate the reaction rates with the driving force free energy and the equilibrium reaction rates [51],

$$\alpha_0 + \alpha_1\alpha = \alpha_{eq} e^{\Delta F/2}$$

$$\beta_1 = \beta_{eq} e^{-\Delta F/2}$$

which implies that

$$log \frac{\alpha_0 + \alpha_1 \alpha}{\beta_1} \frac{\beta_{eq}}{\alpha_{eq}} = \Delta F$$

Additionally, if the free energy F is large enough we can make an assumption that

$$\alpha_0 + \alpha_1 \alpha >> \alpha_{eq}$$

$$\beta_{eq} >> \beta_1$$

With this assumption, the entropy production rate or the power consumption at steady state is finally takes the form,

$$P_{ex}(\alpha) = \sigma = X_T \frac{\beta_{eq}(\alpha_0 + \alpha_1 \alpha)}{\alpha_0 + \alpha_1 \alpha + \beta_{eq}} \Delta F$$

Here, ΔF corresponds to the free energy change of ATP hydrolysis. Thus, entropy would increase as the output increases.

D. Estimating Mutual Information

The dataset used in the study consists of nuclear localization (reported as the ratio of nuclear fluorescence to cytoplasmic fluorescence) of different transcription factor in presence of different stress values. The data is sampled at an interval of 2.5 minutes[12]. The 10 transcription factors used in the study are namely:

msn2, msn4, dot6, tod6, sfp1, maf1, mig1, mig2, hog1, yap1

The three types of stress in which their dynamics is studies are namely.

Carbon Stress, Osmotic Stress, Oxidative Stress

We followed a methodology similar to the one outlined in the referenced paper [12]. The data is normalized by taking the mean and variance of the pre-stress points. Specifically, we consider a trajectory of length 40, comprising 20 pre-stress points and 20 post-stress points, with the point of stress applied at the midpoint of the trajectory. The mean μ and variance σ are calculated from the 20 pre-stress points, ensuring that the pre-stress mean is 0 and the pre-stress variance is 1.

1. *Mutual Information through Decoding*

To calculate Information Gain, we employed a decoding-based technique similar to the one described in the referenced paper [**cite**]. The Information Gain I is defined as:

$$I(X;Y) = \sum_{x,y} p(x,y) \log \frac{p(x,y)}{p(x)p(y)} \tag{1}$$

Direct evaluation of this equation is challenging due to the high dimensionality of $p(x,y)$. Instead, we utilize a parametric form of $p(x,y)$.

The decoding-based estimator operates on individual trajectories, determining whether each trajectory corresponds to a control or stress condition. The classifier functions as a deterministic

mapping $f : x \to \hat{y}$ that assigns a trajectory x to an environment state $\hat{y}$.

The classifier's performance is summarized in a confusion matrix, which shows the counts of correctly and incorrectly classified instances:

		Predicted ($\hat{s}$)	
		$\hat{s_0}$	$\hat{s_1}$
Actual (s)	s_0	$P(\hat{s_0}, s_0)$	$P(\hat{s_1}, s_0)$
	s_1	$P(\hat{s_0}, s_1)$	$P(\hat{s_1}, s_1)$

This matrix is used to estimate the joint probabilities necessary for calculating mutual information. The entries in the matrix are normalized to obtain joint and marginal probabilities, which are then used in the mutual information formula.

The steps of the algorithm are as follows:

1. **Normalize the Data**: For each time point $x_i(t)$, compute the normalized value $\frac{(x_i(t)-\mu)}{\sigma}$. This normalization is based on the first 20 time points before stress is applied and the 20 time points after stress is applied, totaling 40 time points.

2. **Split the Dataset**: Divide the dataset into two halves: the first half as **control** and the second half as **stress**.

3. **Train-Test Split**: Further split the dataset into training (70%) and testing (30%) subsets. Use a **Support Vector Machine (SVM)** to classify the trajectories.

4. **Generate Confusion Matrix**: Post-classification, generate a confusion matrix that shows the count of correct and incorrect classifications.

5. **Normalize Confusion Matrix**: Normalize the confusion matrix to create a probability distribution.

6. **Calculate Information Gain**: Compute the Information Gain I using the normalized probabilities in the mutual information formula given in equation 1

This approach provides an approximate value for the Information Gain using parametric conditional probabilities.

E. Estimated EPR using a neural network model

1. *Data Preparation*

To prepare the data, we followed a procedure similar to that used for Mutual Information analysis. The data was normalized by computing the mean and variance of the pre-stress points. Specifically, we considered trajectories of length 40, comprising 20 pre-stress points and 20 post-stress points.

2. *Algorithm*

In a previous study [32], a novel algorithm is presented for calculating the Entropy Production Rate (EPR) from time series data of biological systems using machine learning techniques. We

adopted the framework outlined in this study to calculate the EPR for the translocation of transcription factors between the cytoplasm and nucleus. This framework provides the EPR directly from the trajectory.

After obtaining a time series of EPR values, we computed their mean to obtain a single EPR value for each transcription factor.

We utilized the (NEEP) representation along with the Variational Estimator, considering them as the default option for handling unknown cases. Our current experimental data only reveals the nuclear localization of the transcription factors at each time point, not the absolute concentration of each state (y1, y2, y3, y4) within our system. To validate our proposed system's behavior, we ideally need the concentration of all states at every time point. To address this limitation, we generated synthetic data by simulating the system using parameter values estimated from the measured temporal changes in the nucleocytoplasmic ratio observed in real data.

F. Parameter Estimation

1. *Data Preparation*

We analyzed the dynamics of transcription factors across 40 time points centered around the stress event for each transcription factor. To enhance model fitting, the trajectories were modified post-stress application by capturing the peak values for all subsequent points. Depending on the nature of the stress, these peak values could represent either the maximum or minimum values observed.

To ensure consistency and comparability, the trajectories were normalized. This was achieved by dividing the modified trajectories by the mean value of the pre-stress region, effectively setting the pre-stress values to 1. This approach allows for a clearer comparison of the transcription factor dynamics before and after stress application, facilitating a more accurate assessment of the stress response.

2. *Proposed Mathematical Model*

The study [35] suggests that transcription factors exhibit oscillatory motion upon the application of stress, influenced by the presence of autoregulatory loops. Figure 4a illustrates our proposed mathematical model. The model comprises eight parameters (k_1 to k_8) and four states (y_1 to y_4), where states y_1 and y_2 represent nuclear states, while y_3 and y_4 represent cytoplasmic states. Stress application is simulated by modifying the constant present in the nucleus, thereby triggering the translocation of transcription factors from the nucleus to the cytoplasm. This model provides a comprehensive representation of the dynamic behavior of transcription factors between the nucleus and cytoplasm, based on the model proposed in the study [35].

The equations governing the states of this model are as follows:

$$\frac{dy_1}{dt} = k_2 y_2 + k_7 y_3 - (k_1 + k_8) y_1, \tag{2}$$

$$\frac{dy_2}{dt} = k_1 y_1 + k_4 y_4 - (k_2 + k_3) y_2, \tag{3}$$

$$\frac{dy_3}{dt} = k_8 y_1 + k_6 y_4 - (k_5 + k_7) y_3, \tag{4}$$

$$\frac{dy_4}{dt} = k_3 y_2 + k_5 y_3 - (k_4 + k_6) y_4. \tag{5}$$

To simulate stress, the parameter k_1 is modified by scaling it with a constant value, inducing shuttling behavior of transcription factors in and out of the nucleus. We estimated the parameters k_1 to k_8 of the chemical reaction using a Genetic Algorithm (GA). Matlab's inbuilt GA toolbox was employed to implement the algorithm, incorporating the modified trajectory in the estimation process. A total of 13 variables were estimated using the GA. These include the reaction constants k_1 to k_8, the initial values of states y_1 to y_4, and the time of application of stress. After each iteration, we generated the predicted trajectory based on the estimated parameter values. The error function for our GA was defined as the Euclidean distance between the original and fitted trajectories:

$$\text{Error} = \sqrt{\sum_i (\text{predicted}(i) - \text{original}(i))^2} \tag{6}$$

To solve the differential equations, we utilized MATLAB's `ode15s` solver, which is efficient for handling stiff differential equations. The graph of the error function is shown in Fig S3. Additionally, Fig S2 illustrates the fitting of the trajectories.

G. Gillespie simulation to generate trajectories

The Gillespie SSA (Stochastic Simulation Algorithm) solver was chosen for this simulation due to its efficiency in handling systems modeled by constant rate mass-action events. Our system was modeled accordingly, and the stress onset was incorporated as a time-dependent event within the simulation. To ensure robustness, we generated 100 independent simulations, each containing 1000 time points, which were then used for further analysis.

With the generated synthetic data, we were able to directly calculate the entropy production rate and flux. This became possible because the simulation provided us with the concentrations of all states in the system at every time point. Additionally, we computed the nucleocytoplasmic ratio over time within each simulated trajectory. To estimate the mutual information, we employed a decoding approach similar to the one used in our original experiment with real data.
To enhance the realism of our simulations, we also generated a set of trajectories that extended beyond a single stress event. This reflects the dynamic nature of cellular processes observed in the experimental data, where stress might be followed by a period of recovery. We achieved this by incorporating a "stress reset" event within the simulation, mimicking the natural fluctuations the system experiences. These trajectories were also used for further analysis.

FIGURES

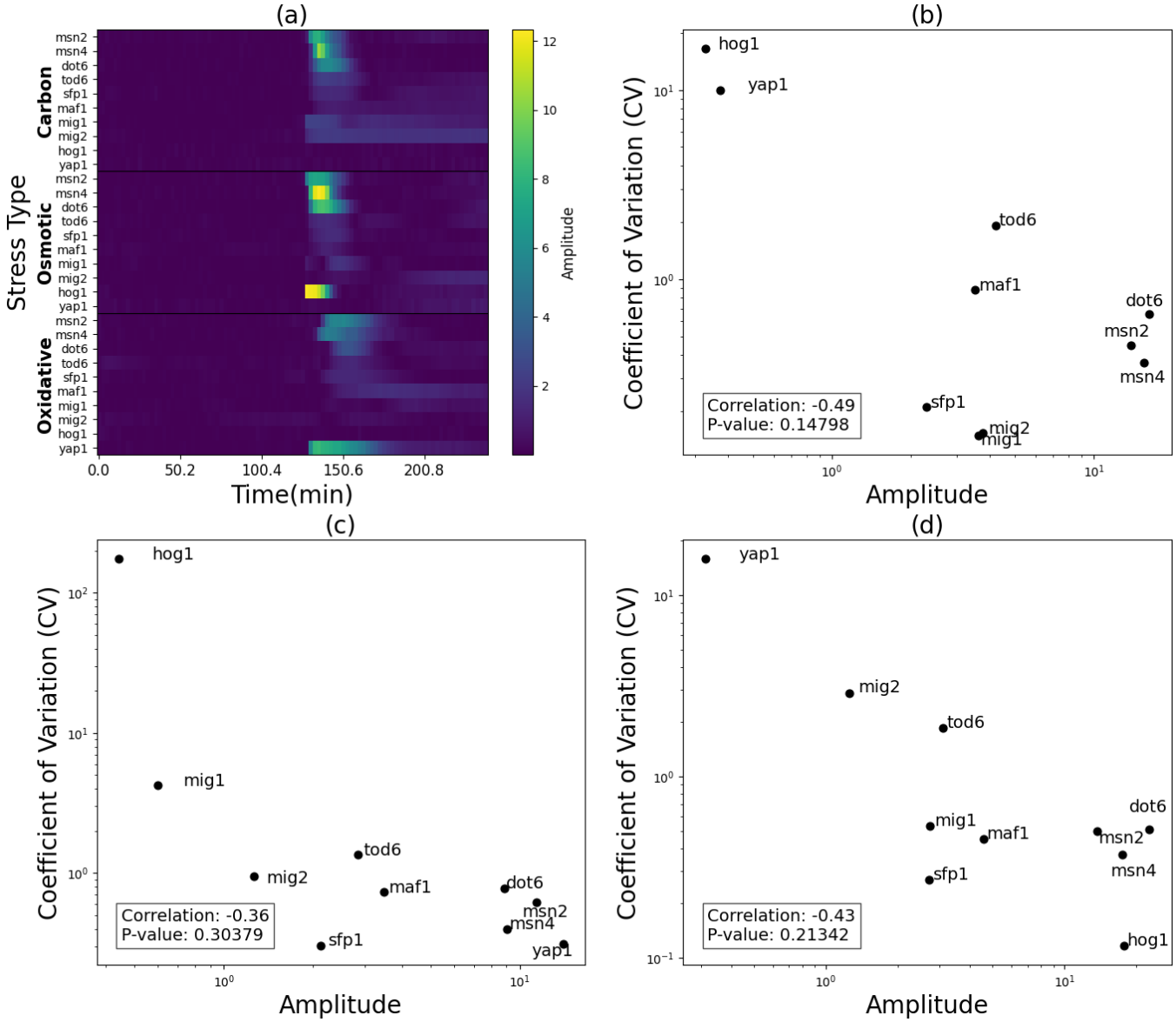

FIG. 1: **High response amplitude reduces fluctuation.**(a)The heat map shows the average trajectories of the amplitude of nuclear-cytoplasmic ratio (NC ratio) over 200 cells for different transcription factors before and after application of the stress under different stress conditions as indicated by an increase in the NC ratio just after the stress is applied.(b) The reduction in fluctuation as the response amplitude is higher, described by the relationship between the $CV = \frac{Variance}{Mean^2}$ of the maximum amplitude for individual single cell trajectories after stress with its $Mean$ calculated over 200 cells for carbon stress (c) the same calculation is done for osmotic stress and (c) oxidative stress

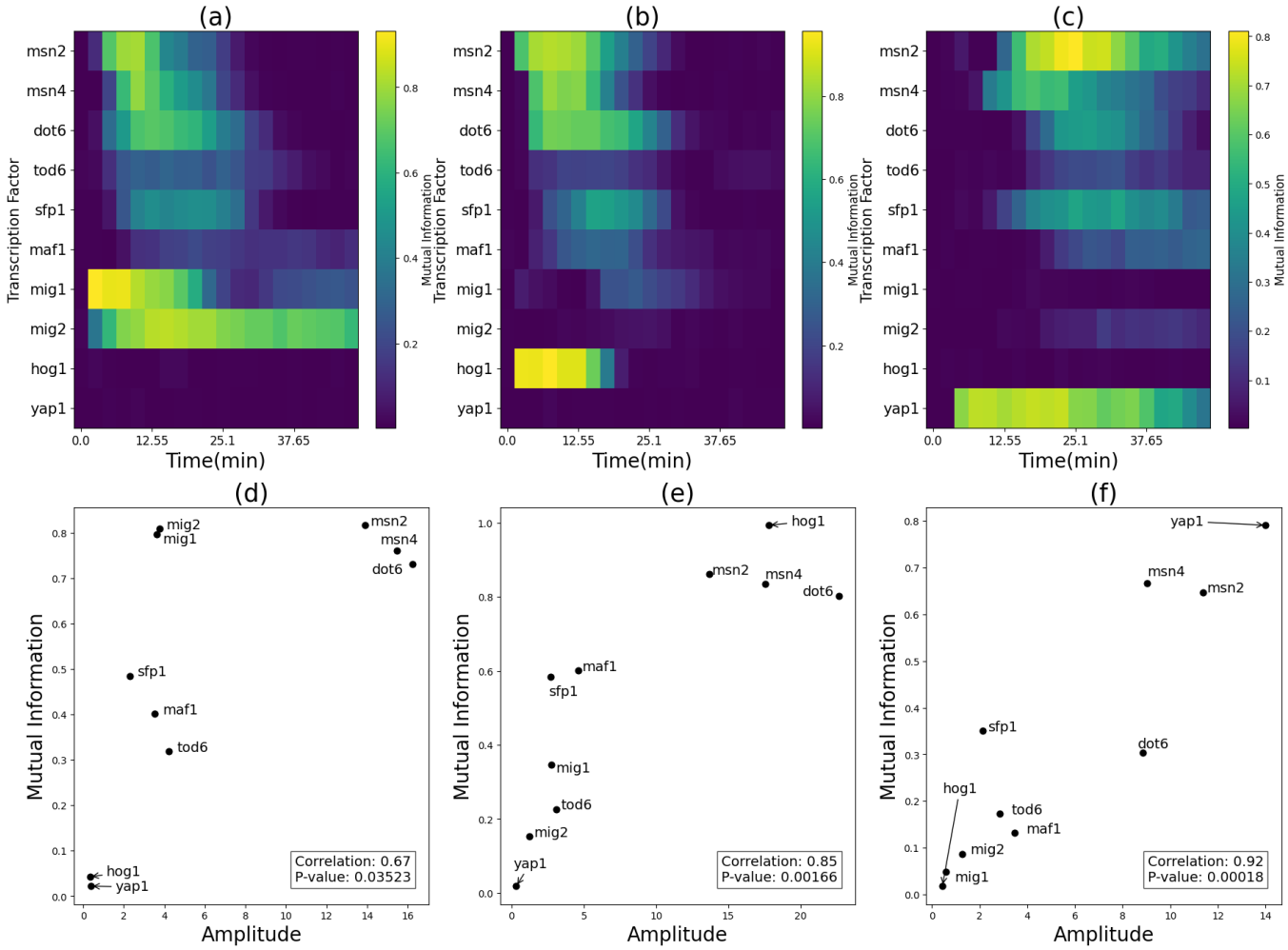

FIG. 2: **Information transmission improves for higher response amplitude.** The mutual information was calculated at the maximum response amplitude for each transcription factor with stress values as the input. (a) The trajectories of mutual information with time for different transcription factors calculated by taking a sliding time window along the response trajectories for carbon stress (b) osmotic stress (c) oxidative stress. The mutual information at maximum response increases with the average response amplitude for the three stress condition namely (d) Carbon (e) Osmotic and (f) Oxidative stress indicated by the positive correlation between mutual information and amplitude

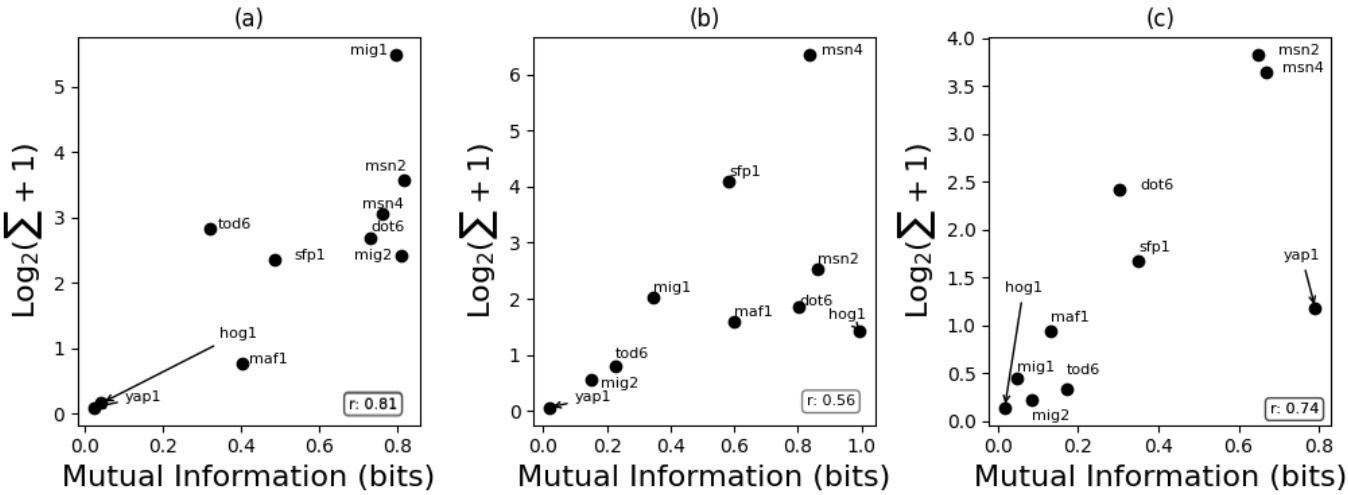

FIG. 3: **Entropy production limits information transmission through the signaling pathways.** The thermodynamic uncertainty relation sets an upper bound on mutual information $I < log(1 + \Sigma)$. The entropy production rate for each trajectory was calculated using a neural network model as described in the main text. The average entropy production over the time to reach the maximum amplitude is determined for each transcription factor at the three different stress conditions. The positive correlation between $log(1 + \Sigma)$ and mutual information for (a) carbon (b) osmotic (c) oxidative stresses suggest the requirement for higher entropy production in reducing the fluctuation leading to higher mutual information. The values of $log(1 + \Sigma)$ is always greater then the mutual information values indicating the corroboration of the inequality

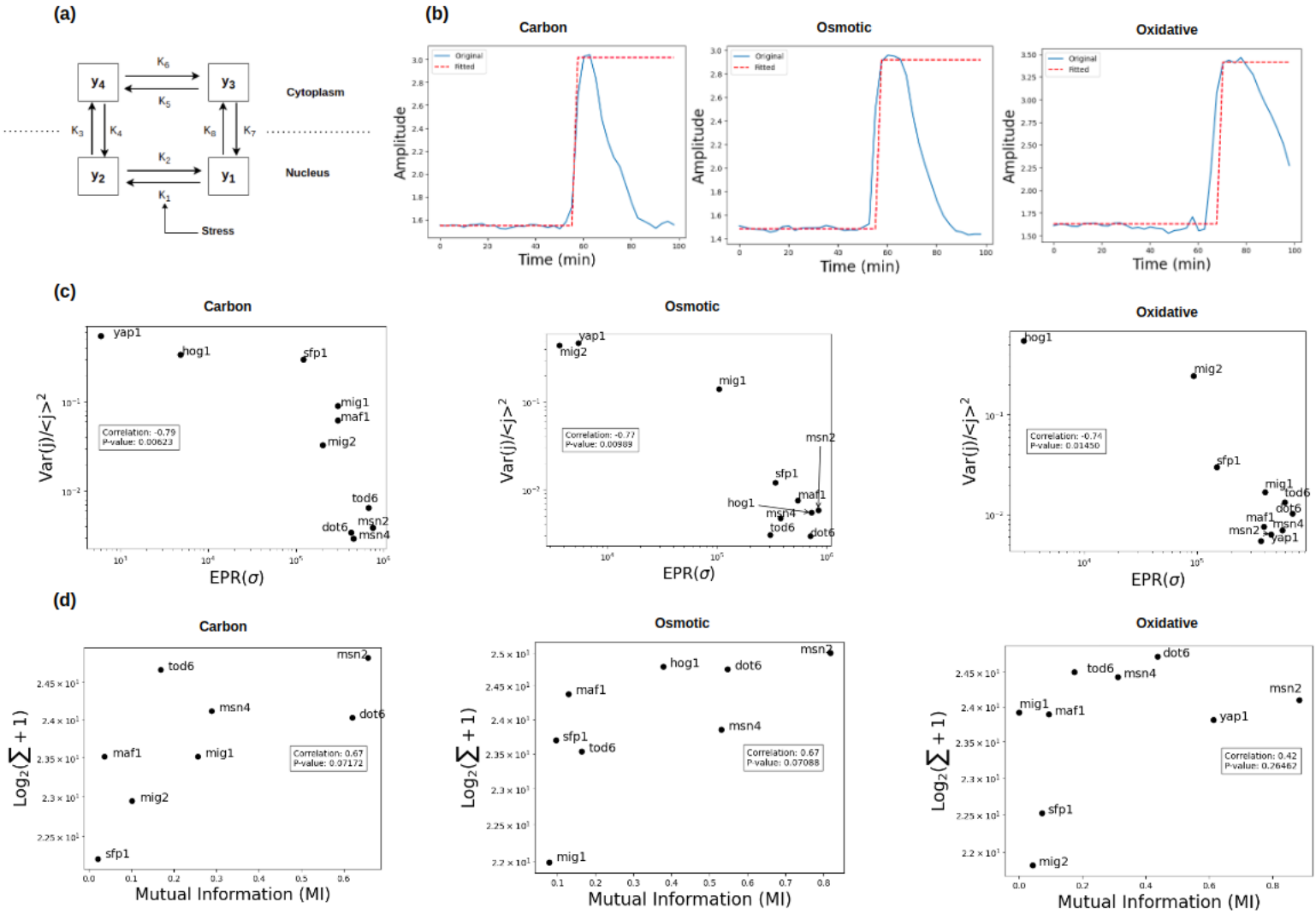

FIG. 4: **The mathematical model displays the limitation of information transmission** (a) The reaction scheme describes the activation of the transcription factor by the application of stress inside the cytoplasm, followed by its localization to the nucleus. Before stress application, the transcription factor concentration remains the same inside the cytoplasm and the nucleus. (b) Original experimental trajectories and the fitted trajectories of NC ratio for the msn2 transcription factor under three different stresses (Carbon. osmotic and oxidative). The pre-stress values of the NC ratio are close to one and increase as stress is applied, reaching a maximum. The model captures only the steady state of the response, excluding subsequent adaptation. Stochastic simulations performed at the estimated parameter values for each transcription factor, calculating the current for each trajectory. (c) The value of $\frac{Var(J)}{<J>^2}$ and the theoretically calculated entropy production rate show a negative correlation for all three stresses, in line with the uncertainty relation. (d) Mutual information and entropy production display a positive correlation for all three stresses, highlighting the role of entropy production in information transmission as suggested by the uncertainty relation.

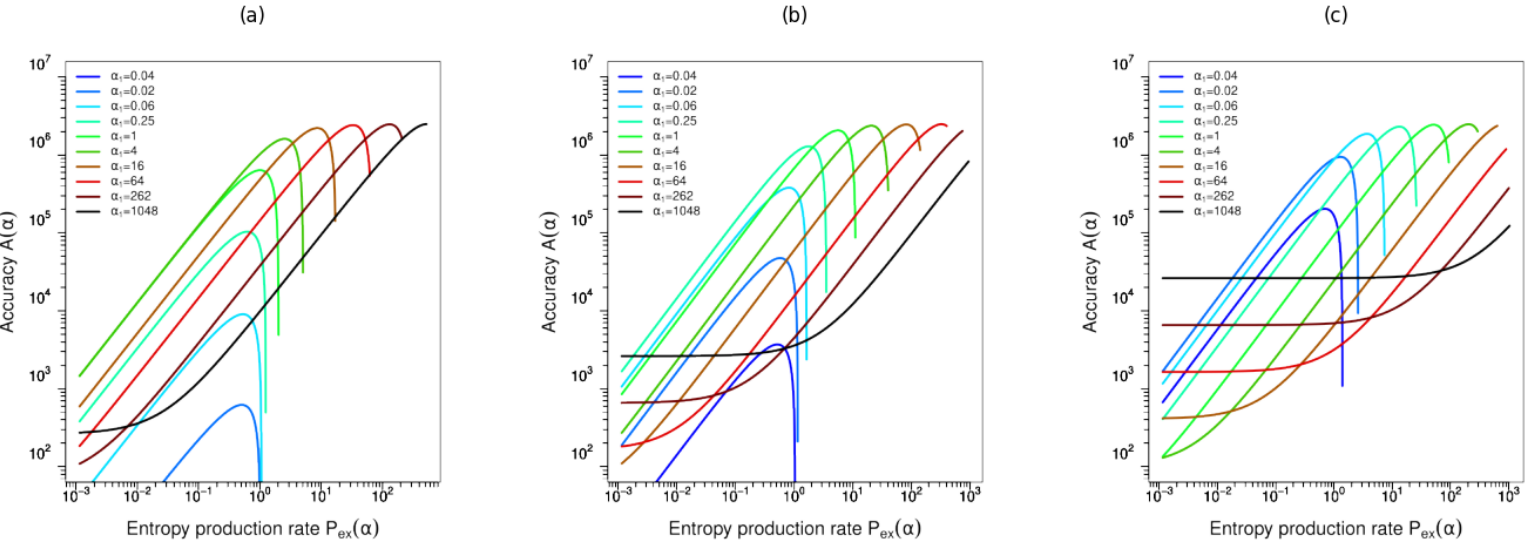

FIG. 5: **Information transmission improves with dissipation rate over a finite range** The accuracy $A(\alpha)$ as a function of the entropy production rate $P_{ex}(\alpha)$ from the analytical expression at different values of the input α as indicated for three values of the activation rates α_1. (a)$\alpha_1 = 1$ (b)$\alpha_1 = 10$ (c)$\alpha_1 = 100$. The accuracy increases with entropy production rate initially but tends to decrease at high entropy production rate indicating the range over which entropy production rate is harnessed to improve the information transmission

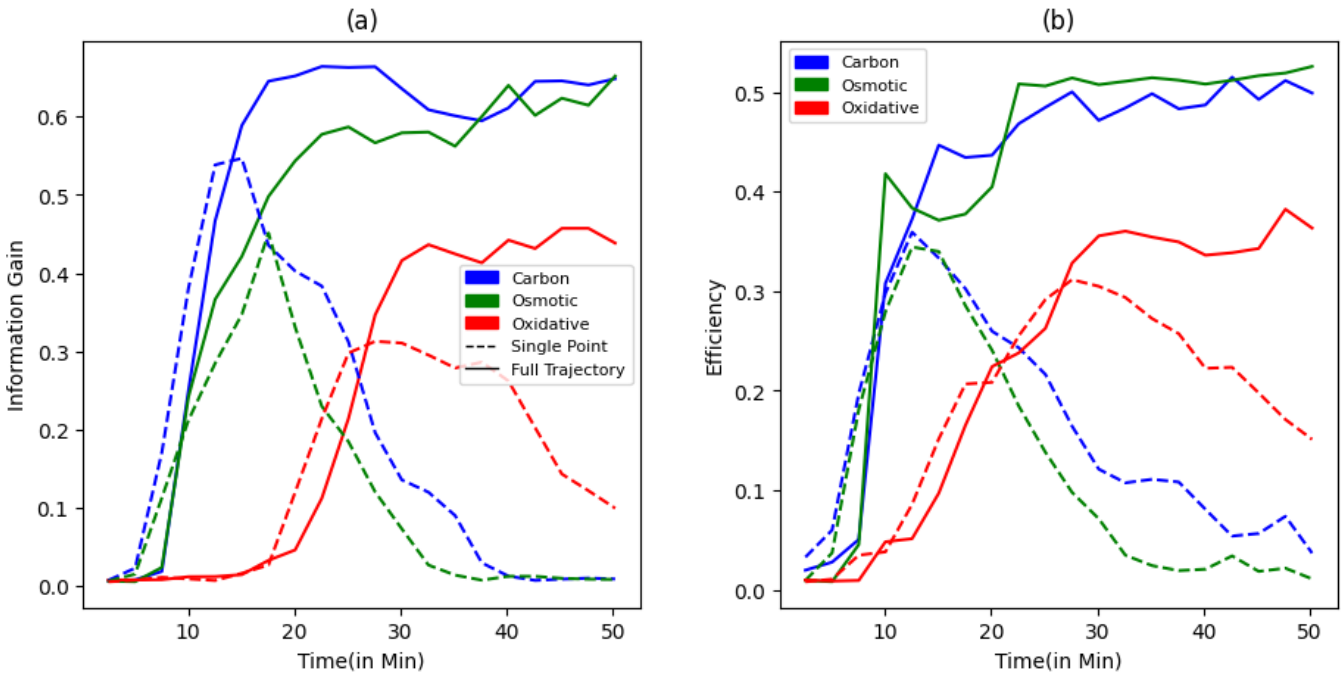

FIG. 6: **Dynamic measurement can improve information transmission and performance efficiency but can not overcome the constraints imposed by thermodynamic uncertainty.**(a) The dynamic mutual information in calculated by varying the length of the trajectory as indicated displaying that the dynamic information increases initially and saturates. The single point information remains lower than the dynamic counterpart for all the stresses. (b) The performance efficiency also exhibits higher value for all the stresses but remains lower than one which is the limit set by thermodynamic uncertainty

REFERENCES

[1] James R Broach. "Nutritional Control of Growth and Development in Yeast". In: *Genetics* 192.1 (Sept. 2012), pp. 73–105. ISSN: 1943-2631. DOI: 10.1534/genetics.111.135731. eprint: https://academic.oup.com/genetics/article-pdf/192/1/73/43425522/genetics0073.pdf. URL: https://doi.org/10.1534/genetics.111.135731.

[2] Jessica Grote, Dagmar Krysciak, and Wolfgang R Streit. "Phenotypic heterogeneity, a phenomenon that may explain why quorum sensing does not always result in truly homogenous cell behavior". In: *Applied and environmental microbiology* 81.16 (2015), pp. 5280–5289.

[3] Theodore J Perkins and Peter S Swain. "Strategies for cellular decision-making". In: *Molecular systems biology* 5.1 (2009), p. 326.

[4] Xue Lei et al. "Biological sources of intrinsic and extrinsic noise in cI expression of lysogenic phage lambda". In: *Scientific reports* 5.1 (2015), pp. 1–12.

[5] Gábor Balázsi, Alexander Van Oudenaarden, and James J Collins. "Cellular decision making and biological noise: from microbes to mammals". In: *Cell* 144.6 (2011), pp. 910–925.

[6] Alexander Anders et al. "Design of a MAPK signalling cascade balances energetic cost versus accuracy of information transmission". In: *Nature communications* 11.1 (2020), pp. 1–10.

[7] Ganhui Lan et al. "The energy–speed–accuracy trade-off in sensory adaptation". In: *Nature physics* 8.5 (2012), pp. 422–428.

[8] Pankaj Mehta and David J Schwab. "Energetic costs of cellular computation". In: *Proceedings of the National Academy of Sciences* 109.44 (2012), pp. 17978–17982.

[9] E Shacter, P Boon Chock, and ER Stadtman. "Energy consumption in a cyclic phosphorylation/dephosphorylation cascade." In: *Journal of Biological Chemistry* 259.19 (1984), pp. 12260–12264.

[10] Jordan M. Horowitz and Todd R Gingrich. "Thermodynamic uncertainty relations constrain non-equilibrium fluctuations". In: *Nature Physics* 16.1 (2020), pp. 15–20. ISSN: 1745-2481. DOI: 10.1038/s41567-019-0702-6. URL: https://doi.org/10.1038/s41567-019-0702-6.

[11] Patrick Pietzonka, Andre C Barato, and Udo Seifert. "Universal bound on the efficiency of molecular motors". In: *Journal of Statistical Mechanics: Theory and Experiment* 2016.12 (Dec. 2016), p. 124004. DOI: 10.1088/1742-5468/2016/12/124004. URL: https://dx.doi.org/10.1088/1742-5468/2016/12/124004.

[12] Alejandro A. Granados et al. "Distributed and dynamic intracellular organization of extracellular information". In: *Proceedings of the National Academy of Sciences* 115.23 (2018), pp. 6088–6093. DOI: 10.1073/pnas.1716659115. eprint: https://www.pnas.org/doi/pdf/10.1073/pnas.1716659115. URL: https://www.pnas.org/doi/abs/10.1073/pnas.1716659115.

[13] Nicolas Brunel and Jean-Pierre Nadal. "Mutual information, Fisher information, and population coding". In: *Neural computation* 10.7 (1998), pp. 1731–1757.

[14] Gašper Tkačik and William Bialek. "Information Processing in Living Systems". In: *Annual Review of Condensed Matter Physics* 7.Volume 7, 2016 (2016), pp. 89–117. ISSN: 1947-5462. DOI: https://doi.org/10.1146/annurev-conmatphys-031214-014803. URL: https://www.annualreviews.org/content/journals/10.1146/annurev-conmatphys-031214-014803.

[15] Nan Hao and Erin K. O'Shea. "Signal-dependent dynamics of transcription factor translocation controls gene expression". In: *Nature Structural & Molecular Biology* 19.1 (Jan. 2012), pp. 31–39. ISSN: 1545-9985. DOI: 10.1038/nsmb.2192. URL: https://doi.org/10.1038/nsmb.2192.

[16] Jeremy E Purvis and Galit Lahav. "Encoding and decoding cellular information through signaling dynamics". en. In: *Cell* 152.5 (Feb. 2013), pp. 945–956.

[17] Jangir Selimkhanov et al. "Accurate information transmission through dynamic biochemical signaling networks". In: *Science* 346.6215 (2014), pp. 1370–1373. DOI: 10.1126/science.1254933. eprint: https://www.science.org/doi/pdf/10.1126/science.1254933. URL: https://www.science.org/doi/abs/10.1126/science.1254933.

[18] Alejandro A. Granados et al. "Distributing tasks via multiple input pathways increases cellular survival in stress". In: *eLife* 6 (May 2017). eLife 2017;6:e21415, e21415. ISSN: 2050-084X. DOI: 10.7554/eLife.21415. URL: https://doi.org/10.7554/eLife.21415.

[19] Robert A Gatenby and B Roy Frieden. "Information theory in living systems, methods, applications, and challenges". In: *Bulletin of mathematical biology* 69.2 (2007), pp. 635–657.

[20] Christoph Adami. "Information theory in molecular biology". In: *Physics of Life Reviews* 1.1 (2004), pp. 3–22.

[21] Andre Levchenko and Ilya Nemenman. "Cellular noise and information transmission". In: *Current opinion in biotechnology* 28 (2014), pp. 156–164.

[22] Shinsuke Uda and Shinya Kuroda. "Analysis of cellular signal transduction from an information theoretic approach". In: *Seminars in cell & developmental biology.* Vol. 51. Elsevier. 2016, pp. 24–31.

[23] Bialek William Petkova MD Tkačik G and Gregor Thomas. "Optimal Decoding of Cellular Identities in a Genetic Network." In: *Cell* 176 (2019), p. 844.

[24] R. Landauer. "Irreversibility and Heat Generation in the Computing Process". In: *IBM Journal of Research and Development* 5.3 (1961), pp. 183–191. DOI: 10.1147/rd.53.0183.

[25] Rolf Landauer. "Information is Physical". In: *Physics Today* 44.5 (May 1991), pp. 23–29. ISSN: 0031-9228. DOI: 10.1063/1.881299. eprint: https://pubs.aip.org/physicstoday/article-pdf/44/5/23/8304036/23_1_online.pdf. URL: https://doi.org/10.1063/1.881299.

[26] Daniel S. Seara et al. "Entropy production rate is maximized in non-contractile actomyosin". In: *Nature Communications* 9.1 (Nov. 2018), p. 4948. ISSN: 2041-1723. DOI: 10.1038/s41467-018-07413-5. URL: https://doi.org/10.1038/s41467-018-07413-5.

[27] Sosuke Ito Naruo Ohga and Artemy Kolchins. "Thermodynamic Bound on the Asymmetry of Cross-Correlations". In: *Phys. Rev. Lett. 131* (2023).

[28] C Van den Broeck J M R Parrondo and R Kawai. "Entropy production and the arrow of time". In: *New J. Phys. 11 073008* (2009).

[29] D. Gupta D. M. Busiello and A. Maritan. "Entropy production in systems with unidirectional transitions". In: *PHYSICAL REVIEW RESEARCH 2, 023011* (2020).

[30] Ken Sekimoto. "Kinetic Characterization of Heat Bath and the Energetics of Thermal Ratchet Models". In: *Journal of the Physical Society of Japan* 66.5 (1997), pp. 1234–1237. DOI: 10.1143/JPSJ.66.1234. eprint: https://doi.org/10.1143/JPSJ.66.1234. URL: https://doi.org/10.1143/JPSJ.66.1234.

[31] Ken Sekimoto. "Langevin Equation and Thermodynamics". In: *Progress of Theoretical Physics Supplement* 130 (Jan. 1998), pp. 17–27. ISSN: 0375-9687. DOI: 10.1143/PTPS.130.17. eprint: https://academic.oup.com/ptps/article-pdf/doi/10.1143/PTPS.130.17/5213518/130-17.pdf. URL: https://doi.org/10.1143/PTPS.130.17.

[32] Shun Otsubo et al. "Estimating time-dependent entropy production from non-equilibrium trajectories". In: *Communications Physics* 5.1 (2022), p. 11. ISSN: 2399-3650. DOI: 10.1038/s42005-021-00787-x. URL: https://doi.org/10.1038/s42005-021-00787-x.

[33] Dominic J. Skinner and Jörn Dunkel. "Improved bounds on entropy production in living systems." In: *Proc Natl Acad Sci U S A* 118.18 (2021), p. 18.

[34] Boyd AB Ray KJ and Guarnieri G. "Thermodynamic uncertainty theorem." In: *Phys Rev E.* 108.5 (2023), p. 054125.

[35] Michel Jacquet et al. "Oscillatory nucleocytoplasmic shuttling of the general stress response transcriptional activators Msn2 and Msn4 in Saccharomyces cerevisiae ". In: *Journal of Cell Biology* 161.3 (May 2003), pp. 497–505. ISSN: 0021-9525. DOI: 10.1083/jcb.200303030. eprint: https://rupress.org/jcb/article-pdf/161/3/497/1533808/jcb1613497.pdf. URL: https://doi.org/10.1083/jcb.200303030.

[36] Tang Y et al. "Quantifying information accumulation encoded in the dynamics of biochemical signaling." In: *Nature* 12.5 (2021), pp. 1272–1280.

[37] Franco Nori Koji Maruyama and Vlatko Vedral. "The Physics of Maxwell's demon and information." In: *Review of Modern Physics 81* 81.1 (2007), p. 18.

[38] Mizraji E. "The biological Maxwell's demons: exploring ideas about the information processing in biological systems." In: *Theory Biosci.* 140.3 (2021), p. 319.

[39] S. Ito and Sagawa T. "Maxwell's demon in biochemical signal transduction with feedback loop." In: *Nat Commun* 6.1 (2015), p. 7498.

[40] Andreas Dechant Takuya Kamijima Sosuke Ito and Takahiro Sagawa. "Thermodynamic uncertainty relations for steady-state thermodynamics". In: *Phys Rev E.* 107.5 (2023), p. L052101.

[41] Mugler A Potter GD Byrd TA and Sun B. "Dynamic Sampling and Information Encoding in Biochemical Networks." In: *Biophys J.* 28.4 (2017), pp. 795–804.

[42] Simon MI Yi TM Huang Y and Doyle J. "Robust perfect adaptation in bacterial chemotaxis through integral feedback control." In: *Proc Natl Acad Sci U S A.* 97.9 (2000), pp. 4649–53.

[43] Christopher C Govern and Pieter Rein Ten Wolde. "Optimal resource allocation in cellular sensing systems". In: *Proceedings of the National Academy of Sciences* 111.49 (2014), pp. 17486–17491.

[44] Bockmayr A Reimers AM Knoop H and Steuer R. "Cellular trade-offs and optimal resource allocation during cyanobacterial diurnal growth. Proc Natl Acad Sci U S A. 2017 Aug 1;114(31)". In: *Proceedings of the National Academy of Sciences* 114.31 (2017), E6457–E6465.

[45] Schroeder S Hu X-P and Lercher MJ. "Proteome efficiency of metabolic pathways in Escherichia coli increases along the nutrient flow." In: *mSystems* 8.5 (2023), e0076023.

[46] Mateescu EM Scott M Klumpp S and Hwa T. "Emergence of robust growth laws from optimal regulation of ribosome synthesis. Mol Syst Biol. 2014 Aug 22;10(8):747." In: *Mol Syst Biol.* 10.8 (2014), p. 747.

[47] Takahiro Hatano and Shin-ichi Sasa. "Steady-state thermodynamics of Langevin systems". In: *Physical review letters* 86.16 (2001), p. 3463.

[48] David A Sivak and Gavin E Crooks. "Thermodynamic metrics and optimal paths". In: *Physical review letters* 108.19 (2012), p. 190602.

[49] Subhaneil Lahiri, Jascha Sohl-Dickstein, and Surya Ganguli. "A universal tradeoff between power, precision and speed in physical communication". In: *arXiv preprint arXiv:1603.07758* (2016).

[50] T. Tomé and M. J. de Oliveira. "Stochastic thermodynamics and entropy production of chemical reaction systems." In: *Journal of Chemical Physics* 148.22 (2018), p. 224104.

[51] JM Horowitz and JL England. "Spontaneous fine-tuning to environment in many-species chemical reaction networks." In: *Proc Natl Acad Sci U S A* 114.29 (2017), pp. 7565–7570.

APPENDIX

(a)

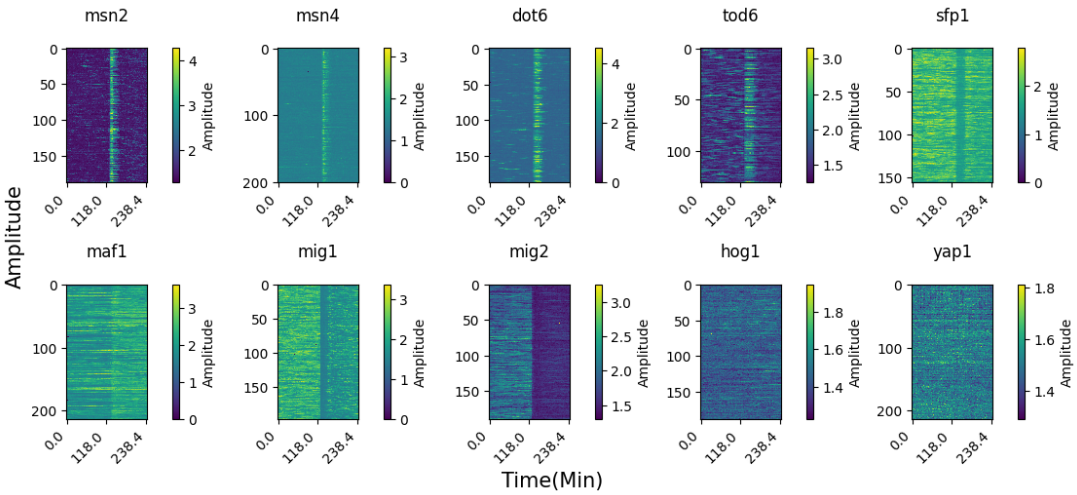

(a) Carbon

(b)

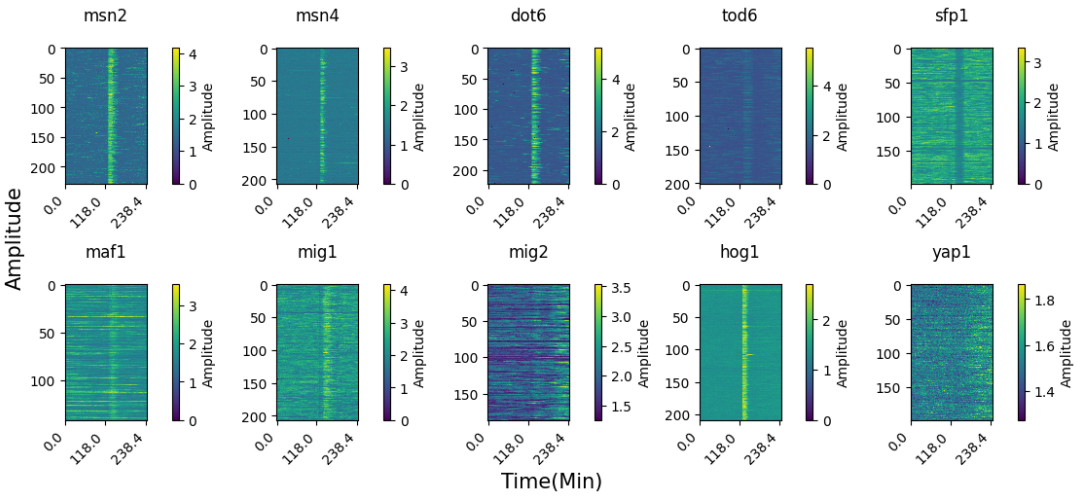

(b) Osmotic

(c)

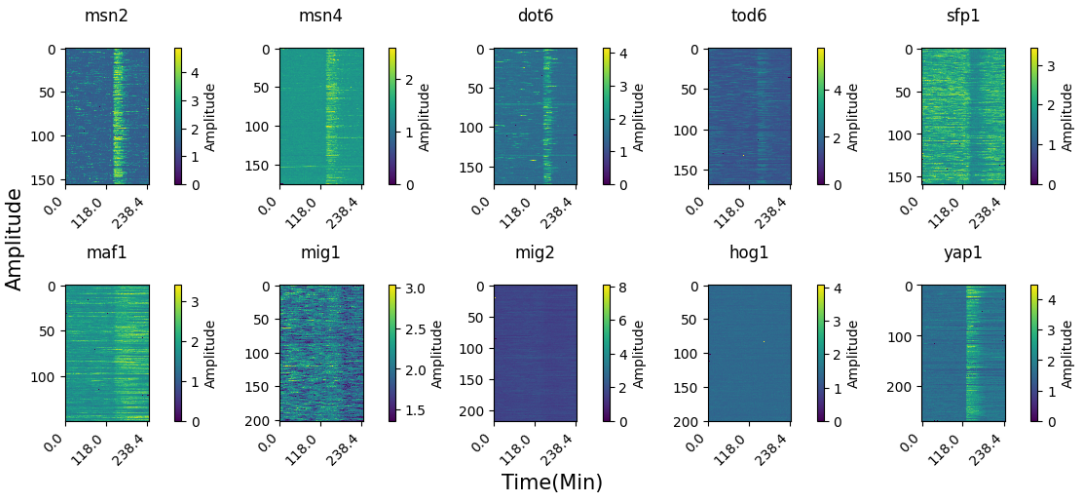

(c) Oxidative

Fig. S1: Trajectories of NC ratio inside individual cells for different transcription factors before and after different stress conditions: (a) Carbon, (b) Osmotic, and (c) Oxidative.

(a)

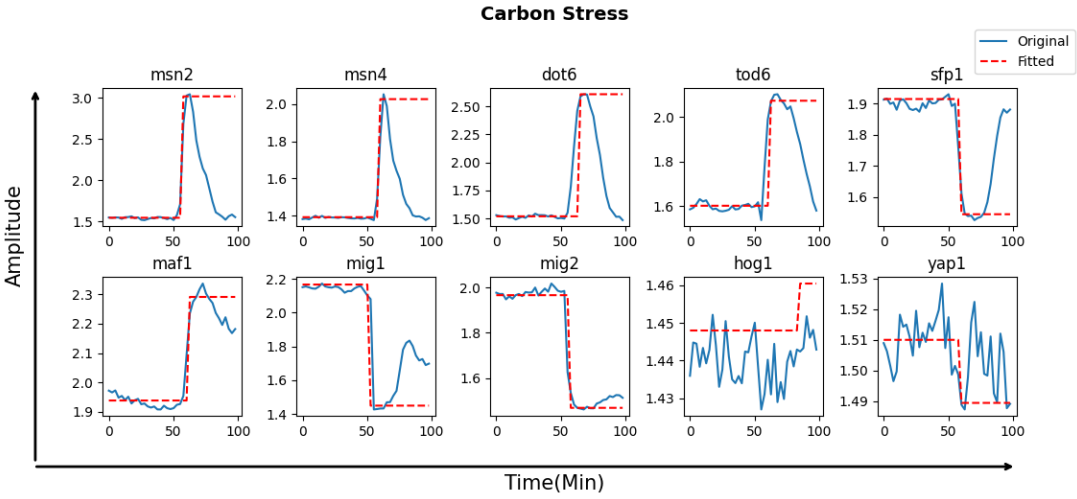

(a) Carbon Curve Fit

(b)

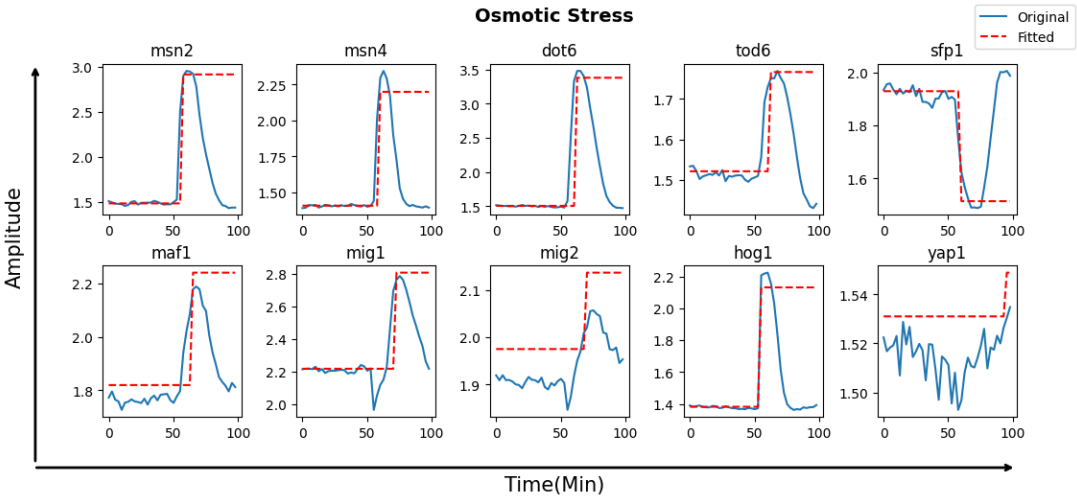

(b) Osmotic Curve Fit

(c)

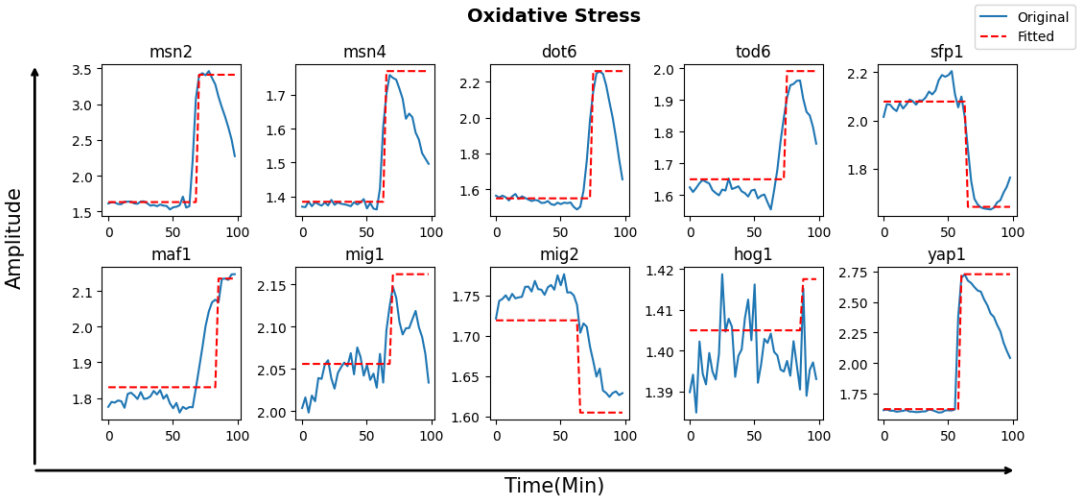

(c) Oxidative Curve Fit

Fig. S2: Average trajectories of NC ratio for different transcription factors in blue before and after different stress conditions: (a) Carbon, (b) Osmotic, and (c) Oxidative and the corresponding trajectories in red fitted by the genetic algorithm

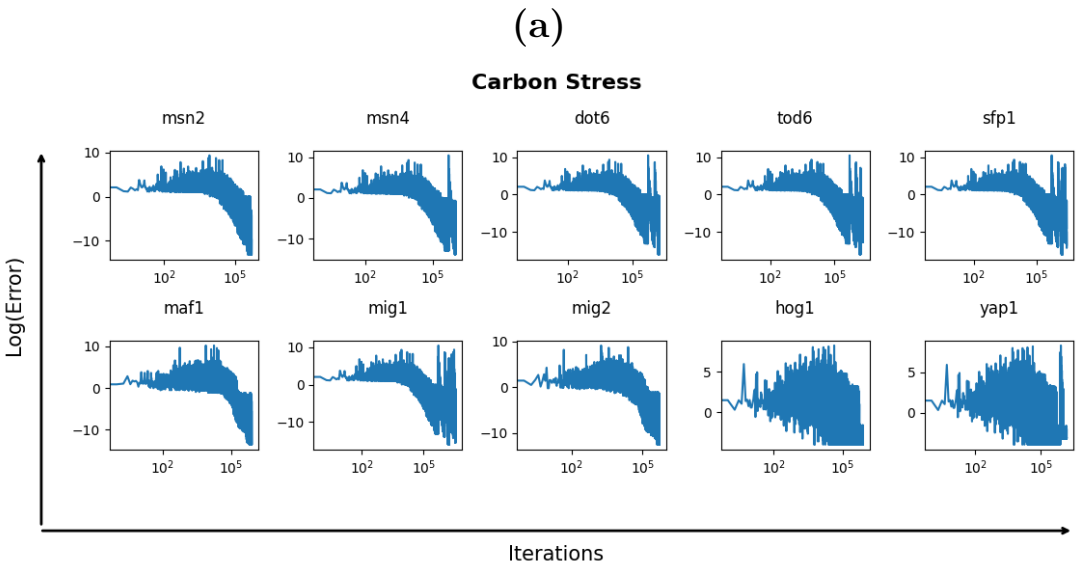

(a) GA Error - Carbon

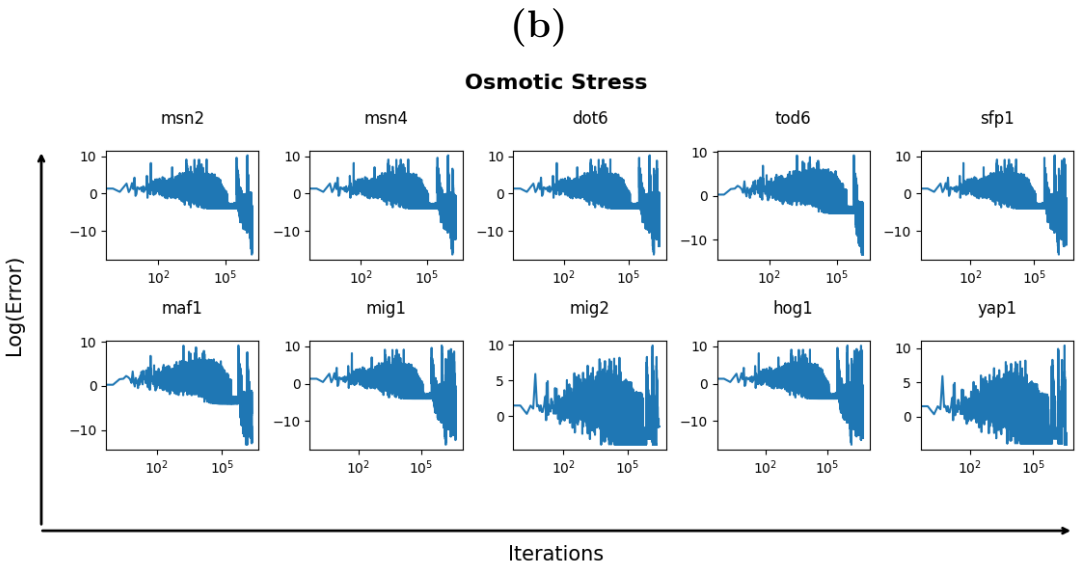

(b) GA Error - Osmotic

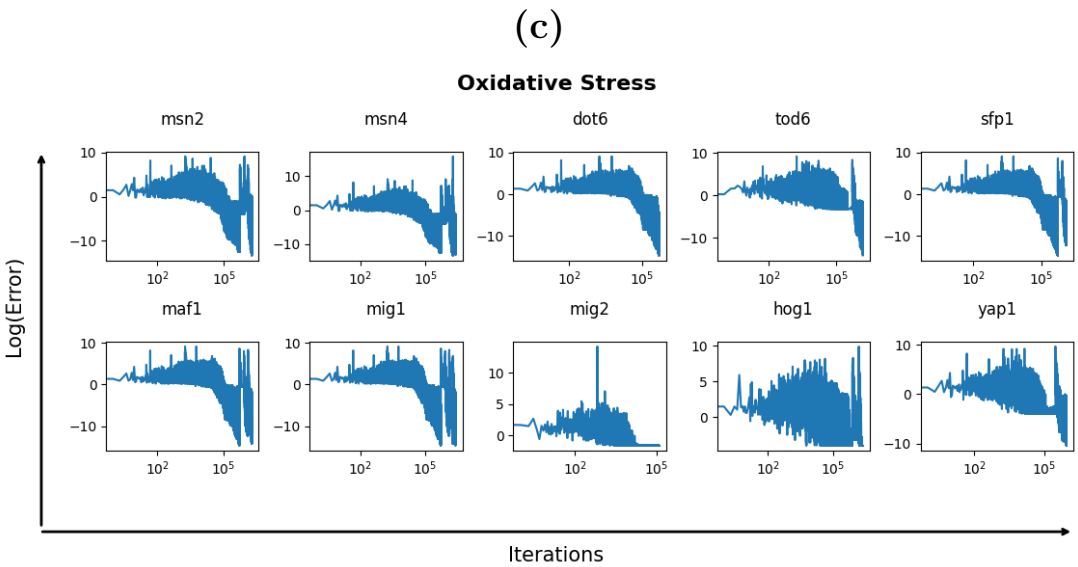

(c) GA Error - Oxidative

Fig. S3: Genetic Algorithm (GA) Error Analysis for different conditions: (a) Carbon, (b) Osmotic, and (c) Oxidative as indicated for different transcription factor trajectories